

## Comprehensive Computational Approach to Determine Novel Ligands for Phosphodiesterase 10 (Pde10a) Inhibitors

Reena Singh<sup>1</sup>, Anjani Kumar Tiwari<sup>2</sup>, Shivani Mishra<sup>3</sup>, Ravendra Singh Chauhan<sup>4</sup>, Rajesh Kumar Yadav<sup>5</sup> and Dushyant Kumar<sup>6</sup>, Devyani Barodh<sup>7</sup>, Narendra Kumar Sharma<sup>8</sup>

<sup>1, 3, 5, 4</sup> Department of Chemistry Shri Jai Narain Misra Post Graduate Degree College Lucknow, Uttar Pradesh 226001, India

<sup>2</sup> Department of Chemistry, Babasaheb Bhimrao Ambedkar University (A Central University), Lucknow, Uttar Pradesh 226025, India

<sup>6 & 7</sup> College of Homeopathy, Madhav University Pindwara, Sirohi, Rajasthan - 307026, India

<sup>8</sup> Associate Professor, Faculty of Basic Science, Madhav University Pindwara, Sirohi, Rajasthan - 307026, India

---

### ARTICLE DETAILS

**Research Paper**

**Accepted:** 28-03-2025

**Published:** 10-04-2025

**Keywords:**

*Phosphodiesterase (PDE10A), ADME, molecular docking & QSAR*

---

### ABSTRACT

In the quest for novel therapeutics for neuro inflammatory conditions, targeting PDE10A has emerged as a promising approach. An effective therapeutic strategy for treating schizophrenia involves targeting PDE10A. The protein structure was prepared in order to complete docking with 2D structure of 32 molecules designed using Chem Draw 2D software and optimized by applying the force field. Thirty two new ligands were generated by substituting various groups in to a lead pharmacophores Benzyl (1-1,2-Dioxo-1-(pyridin-2Ylmethyl) amino)hexan-3-yl) amino) – 4 – methyl – 1 – Oxopentan – 2 - yl) carbamate. A series of compounds were prepared by varying the substituent's based on inductive effect, positive and negative mesomeric effect. In the next step we used Flex docking software and Swiss ADMET prediction tools, to assess the binding affinity and pharmacokinetics of 32 selected molecules. Molecular docking analysis revealed that the most potent inhibitor formed hydrogen bonds and exhibited hydrophobic interactions within the active pocket of the PDE10A complex. These

findings align with the QSAR model, further validating the potential of this compound as a strong PDE10A inhibitor. We identified top poses with optimal binding properties and gained a deeper understanding of the molecular interactions driving their binding affinity. The binding affinity were found in the range of -31 to -55. The Ligand efficiencies span a range of 0.19 to 0.34 with higher values indicating a more efficient binding interaction. The contributions of the hydrogen bond, Vander Waals, and  $\pi$ - $\pi$ -interaction were included in the dockings core with the residues HIS-515, ASN-582, TYR-603, TYR-683, TYR-514, GLN-714, and GLN-716. These finding showed the future importance of these molecules for PDE10 targeting.

---

**DOI : <https://doi.org/10.5281/zenodo.15484995>**

---

## **Introduction**

Drug design has made extensive use of experimental and high-throughput screening techniques over the past few decades. Traditional methods for finding new therapeutic medications were more costly, time-consuming, and ineffective. Modern drug's research and development takes a least of time, efforts, and money. In initial a compound is lack of responsible for clinical and biological features frequently hinders the development of a novel the rapeutic candidate [1,2]. Drug design is the inventive process of discovering novel medications based on the understanding of a biological target [3].

The discovery of novel pharmaceuticals with potential therapeutic applications is one of the pharmaceutical industry's most complex and demanding processes. The discovery of novel medicinal compounds requires millions of dollars and man-hours. Rational drug design has been a fantasy for decades because the action of a medicine is determined by a variety of parameters such as bioavailability, toxicity and metabolism [4,5].

Computer simulation of a potential preferred orientation for the receptor's ligand binding site developed an in silico approach that successfully combines the prediction of physiochemical and pharmacokinetic features, molecular docking, ADME, and the search for new potential therapeutic molecules on the PDE10A receptor [6-8]. Among the phosphodiesterase at least eleven distinct PDE families found, phosphodiesterase PDE10A is known for its effectiveness in treating schizophrenia (SCZ)



in human settings in animal models if anyone known the precise molecular structure of the target (protein and receptor) then we can use a CADD method for drug design perfectly fitting ligand using the drug design consists of idea, knowledge and tools [9-11]. Antipsychotics are the primary medication. For example, motion, disturbance, dizziness, cardiac arrhythmia, and weight gain that raises the risk of diabetes and cardiovascular disease [12]. The molecular docking analysis of the most potent inhibitor revealed that hydrogen bond formation and hydrophobicity participated in the binding interaction PDE10A complex active pocket, and these findings are in line with this [13-15].

In the present study PDE10A, has a 3D structure that was obtained from protein data bank under the code 3QPP. This code corresponds to the 3D structure of the PDE 10A in complex with a co-crystallized inhibitor that has the code 3QPP. Since PDE10A is a homodimeric enzyme, we eliminate one of its chains which was then separated from its inhibitor (3QPP) to preserve only the enzyme with a free active site [16-18]. The brain region known as striatal medium spiny neurons of the basal ganglia complex which is thought to have a strong reaction to external executive behaviours, has the highest density of PDE10A (Phosphodiesterase) expression [19,20]. The crystal of PDE10A complex with 3QPP was determined X-ray diffraction of 1.80 angstrom. The classification of phosphodiesterase structure is based on hydrolase organism, the R value of the structure which indicates the quality of structure fit between the observed and calculated data R value 0.2010. R value is work on 0.184 and R value observed 0.186. The strongest inhibitor's molecular docking analysis these results align with the revelation that hydrogen bond formation and hydrophobicity played a role in the binding interaction of the PDE10A complex active pocket [21].

## Methodology

**Ligand Preparation** - The ligand structure was produced using lead IT software via receptor preparation each receptors active site was shown in order to complete docking following our earlier work. The 2D structure of 32 molecules was designed using Chem Draw 2D software and then optimized by applying the force Field (mmff94) using Chem3D software.

Thirty two new ligands were generated by substituting various groups into a lead pharmacophore Benzyl (1-((1,2-dioxo-1-((pyridin-2-ylmethyl)amino)hexan-3-yl)amino)-4-methyl-1-Oxopentan-2-yl)carbamate.

The substituents were selected from three series: inductive effect (strong, medium, and weak), positive mesomeric effect (strong, medium, and weak), and negative mesomeric effect. The goal was to create

stable ligands by strategically placing groups with negative effects at positions with high electron density and groups with positive effects at positions with low electron density.

**Table-Ligand structures on the basis of stability of R1, R2, R3 & R4**

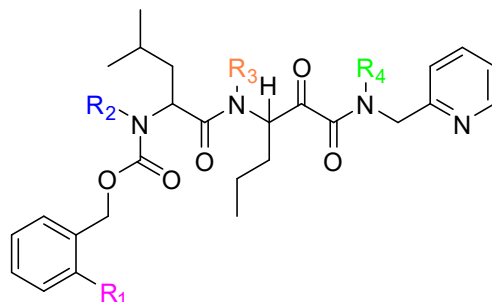


**Fig.1**

S.NO	R1	R2	R3	R4	Formula
1.	-	H	H	H	C <sub>26</sub> H <sub>34</sub> N <sub>4</sub> O <sub>5</sub>
2.	-	H <sub>3</sub> C	H	H	C <sub>27</sub> H <sub>36</sub> N <sub>4</sub> O <sub>5</sub>
3.	-	H <sub>3</sub> C	CH <sub>3</sub>	H	C <sub>28</sub> H <sub>38</sub> N <sub>4</sub> O <sub>5</sub>
4.	-	H <sub>3</sub> C	CH <sub>3</sub>	H	C <sub>29</sub> H <sub>40</sub> N <sub>4</sub> O <sub>5</sub>
5.	OH	CH <sub>3</sub>	CH <sub>3</sub>	H	C <sub>29</sub> H <sub>40</sub> N <sub>4</sub> O <sub>6</sub>
6.	OH	H	H	H	C <sub>26</sub> H <sub>34</sub> N <sub>4</sub> O <sub>6</sub>
7.	OH	H <sub>3</sub> C	H	H	C <sub>27</sub> H <sub>36</sub> N <sub>4</sub> O <sub>6</sub>
8.	OH	H <sub>3</sub> C	CH <sub>3</sub>	H	C <sub>28</sub> H <sub>38</sub> N <sub>4</sub> O <sub>6</sub>
9.	OH	H	H	H	C <sub>26</sub> H <sub>34</sub> N <sub>4</sub> O <sub>6</sub>
10.	OH	H <sub>3</sub> C	H	H	C <sub>27</sub> H <sub>36</sub> N <sub>4</sub> O <sub>6</sub>
11.	OH	H <sub>3</sub> C	CH <sub>3</sub>	H	C <sub>28</sub> H <sub>38</sub> N <sub>4</sub> O <sub>6</sub>
12.	OH	H <sub>3</sub> C	CH <sub>3</sub>	CH <sub>3</sub>	C <sub>29</sub> H <sub>40</sub> N <sub>4</sub> O <sub>6</sub>
13.	CH <sub>3</sub>	H	H	H	C <sub>27</sub> H <sub>36</sub> N <sub>4</sub> O <sub>5</sub>
14.	CH <sub>3</sub>	H <sub>3</sub> C	H	H	C <sub>28</sub> H <sub>38</sub> N <sub>4</sub> O <sub>5</sub>
15.	CH <sub>3</sub>	H <sub>3</sub> C	CH <sub>3</sub>	H	C <sub>29</sub> H <sub>40</sub> N <sub>4</sub> O <sub>5</sub>
16.	CH <sub>3</sub>	H <sub>3</sub> C	CH <sub>3</sub>	CH <sub>3</sub>	C <sub>30</sub> H <sub>42</sub> N <sub>4</sub> O <sub>5</sub>
17.	H <sub>2</sub> N	H	H	H	C <sub>26</sub> H <sub>35</sub> N <sub>5</sub> O <sub>5</sub>



18.	H2N	H3C	H	H	C27H37N5O5
19.	H2N	H3C	H3C	H	C28H39N5O5
20.	H2N	H3C	H3C	H3C	C29H41N5O5
21.	O2N	H	H	H	C26H33N5O7
22.	O2N	H3C	H	H	C27H35N5O7
23.	O2N	H3C	H3C	H	C28H37N5O7
24.	O2N	H3C	H3C	H3C	C29H39N5O7
25.	SO3	H	H	H	C26H34N4O8S
26.	SO3	H3C	H	H	C27H36N4O8S
27.	SO3	H3C	H3C	H	C28H38N4O8S
28.	SO3	H3C	H3C	H3C	C29H40N4O8S
29.	Br	H	H	H	C26H33BrN4O5
30.	Br	H3C	H	H	C27H35BrN4O5
31.	Br	H3C	H3C	H	C28H37BrN4O5
32.	Br	H3C	H3C	H3C	C29H39BrN4O5

## Protein Preparation

Protein was selected from the PDB database on the RCSB website and downloaded in PDB format. The protein structure was then prepared by removing water molecules leaving only the protein atoms. Molecular docking was performed using Lead IT started by downloading a protein structure from the RCSB website and uploading it to the software. We had removed water molecules and then load the ligand molecule in mol-2 format. Run the docking simulation and identify the top 10 poses based on the green indicators of success full docking. Finally, evaluate the binding affinity of each pose using the G values, which indicates stronger binding with lower values.

## ADMET

The identification of possible drug likeness behavior was facilitated by the using Swiss ADME web tool ([www.swissadme.ch](http://www.swissadme.ch)) for in silico prediction of various pharmacokinetic, physicochemical, and drug-like aspects of compounds.



Swiss ADME software was utilized for ADMET profiling. The drawing tool was accessed by selecting the draw molecule tap on the home page of the Swiss ADME website. The chemical that was drawn utilizing the submit molecule to the Swiss ADME was chosen. The ability to generate structure from SMILES (Simplified Molecular Input Line Entry Specification) is included in Chem Sketch's free edition. Only a small percentage of common users appear to be using the SMILES feature. SMILES structure can also be drawn from Chem Sketch's. The molecules ADMET characteristics such as its molecular weight, log p (partition coefficient), log s (solubility), Lipinski rule of five hydrogen bond the blood-brain barrier is the donor-acceptor hydrogen bond donor.

## QSAR

Star Drop software used for QSAR studies, here we followed a structured workflow (Shown in fig. 1). First, we format our dataset and import it into Star Drop, selecting relevant descriptors based on molecular properties then we apply the Lipinski rule of five to assess drug-likeness and generate as core. Graphical visualization helps us identify patterns and correlations (Shown in fig. 2). Finally, we compare prepared descriptor with the original data set to uncover relationships and predictive models. The Lipinski rule was used to calculate the number of atoms type personalities and molecule properties such as long-range molecular weight and polar surface area using experimental octanol/water and model-derived molecule. The star Drop model is based on an external data collection of experiments related to drug development solubility permeability and water distribution corporation value of jobs. Star Drop categories acid base materials and neutral categories based on characteristics but does not attempt to forecast Pka.

## Result and Discussion

### [A] – Docking studies of selected compound

Molecular docking is one of the most significant approaches. Drug targets, including as proteins, nucleic acids, lipids, and ligands, interact with one another among themselves in the study of molecular docking and modeling. To reduce the free energy of the entire system, molecular docking seeks to optimize the conformation of the protein and the ligand as well as the relative orientation between them. This paper reveals that many facts of molecular docking, such as the fundamental docking stages, interaction kinds, and software tools along with their methods and uses. This study aimed to predict the binding affinity of series 1 and 2 compounds to the PDE10A protein. To achieve this, we obtained the 3QPP structure and



investigated how the ligands interact with the binding site, shedding light on the molecular mechanisms underlying their binding affinity. Total of sixteen selected compounds were assessed for their ability to bind efficiently to the 3QPP protein binding site. Using the HYDE process, we predicted the binding affinity of each compound by calculating the realistic free energy of binding. This approach considers various aspects of the docking analysis and priorities of compounds is based on their binding efficiency. As a result, we identified top candidates with optimal binding properties and gained a deeper understanding of the molecular interactions driving their binding affinity. The binding affinity values span a range of -31 to -55 with more negative values signifying stronger binding interactions. In other words, molecules with binding affinity values closer to -55 exhibit stronger binding to the target protein, while those with values closer to -31 exhibit relatively weaker binding. The ligand efficiencies span a range of 0.19 to 0.34, with higher values indicating a more efficient binding interaction. The dockings cores enable the ranking of ligands according to their binding affinity to the target protein, with higher-ranked ligands exhibiting stronger binding interactions and lower-ranked ligands displaying weaker interactions.

In this paper we have taken 32 compounds out of them we have proceed with 16 leading compounds which have shown best results mentioned with more negative docking scores such as L-15 (-23.5423) and L-16 (17.7367), Show better binding affinity to the target protein while ligand with less docking scores such as L-13 (-4.1237), L-14 (-9.3494) and L-10 (-10.8505), show weaker binding Affinity. The ligands were renamed as L-01 to L-16 on the basis of above mentioned docking result as says.

The ligand efficiencies provide a measure of how efficiently the ligand binds to the target protein based on its size. Ligand with higher ligand efficiencies such as L-01 (0.34), L-02 (0.33) and L-03 (0.27) bind more efficiently to the target protein while ligand with lower ligand efficiency such as L-15 (0.19) have poor binding affinity. Molecules in the first category are considered the most promising among all 16 molecules. Our priority criteria rank molecules as follows:

Docking score as the primary factor, followed by binding affinity, and then ligand efficiency. Therefore, molecules with high docking scores, strong binding affinity, and optimal ligand efficiency are considered the best pose for leading compound.

**Table** Docking results of PDE10A derivatives with PDBID:3QPP.

Compound	Compound	HS(K DS	LE	MATCH	LIPO	AMBIG	CLASH	ROT	MAT	
und	d	J/							CH	
	Renamin	mol								
	g	)								
16.	L-01	-55	-11.1346	0.34	-12.4974	-22.7217	-10.7231	11.2076	18.2000	14
04.	L-02	-52	-10.9057	0.33	-16.8569	-21.4980	-10.6295	14.4788	18.2000	22
32.	L-03	-45	-10.1563	0.27	-15.5450	-17.4483	-08.4666	07.7035	18.2000	12
23.	L-04	-44	-11.6967	0.26	-15.6102	-19.4272	-13.1708	12.9115	18.2000	16
28.	L-05	-43	-10.9822	0.25	-18.4653	-18.4653	-15.0513	17.7449	19.6000	21
24.	L-06	-42	-11.0062	0.24	-15.6136	-17.0026	-09.7416	09.7416	18.2000	11
10.	L-07	-37	-12.9344	0.00	-24.9548	-8.9528	-10.1994	06.1726	19.6000	14
31.	L-08	-40	-10.9404	0.25	-15.9424	-15.3725	-07.3804	04.1548	18.2000	08
02.	L-09	-37	-12.2669	0.25	-16.9625	-15.2305	-06.9038	03.2299	18.2000	13
15.	L-10	-35	-10.8505	0.22	-15.5319	-21.1174	-13.0822	15.2810	18.2000	15
20.	L-11	-35	-12.0574	0.22	-18.3225	-16.5157	-09.2594	08.4402	18.2000	14
14.	L-12	-34	-17.7367	0.22	-17.1509	-20.7366	-09.5200	06.0707	18.2000	17
08.	L-13	-34	-04.1237	0.22	-13.4436	-11.7266	-09.7034	05.7499	19.6000	09
05.	L-14	-32	-09.3499	0.19	-15.7683	-15.4680	-07.7622	04.6485	19.6000	08
18.	L-15	-31	-23.5423	0.20	-27.9236	-17.6957	-09.7716	08.2485	18.2000	25
03.	L-16	-28	-17.9775	0.18	-30.0615	-12.2561	-08.5816	09.3217	18.2000	27

Docking Score (DS), hyde score (HS), ligand efficiency (LE),lipophilicity contact area (LIPO), ambiguous score (AMBIG);clash penalty score (CLASH).

#### [B] – Binding interaction and interpretation of selected compound -

The contributions of the hydrogen bond, vander Waals interaction, and  $\pi$ - $\pi$ -interaction were included in the docking score. With this residues HIS-515, ASN-582, TYR-603, TYR-683, TYR-714, GLN -715, GLN -716. Chemical structure forms hydrogen bond interactions. As a result of the strong electrostatic interactions created between the hydrogen atoms of the ligand and the receptor, these hydrogen bonds



help to stabilise the ligand-receptor complex. The opposite charges between the ligand and the receptor cause these attractive charge interactions, which promote beneficial electrostatic interactions and increase the ligand's binding affinity. With these PHE-686, PRO-702, GLU-711 this interacts hydrophobically. In order to maintain the stability of ligand-receptor complexes, hydrophobic interactions are essential enabling favorable interactions.

**Table** Interaction results of PDE10 Aderivatives with PDBID:3QPP.

Compo und	H-Bond	SaltBridge	HBI(Pi-Pi bond)	VanderWaals
L-01	TYR-683		PHR-686 PRO-702	HIS-515SER-561LEU-625PHE-629SER-667VAL-668 ALA-679MET-704LYS-708 ARG-709GLU-711 VAL-712GLY-715ALA722
L-02			PHE-686 PRO-702 GLU-711	HIS-515SER-561LEU-625PHE-629LEU-665TYR-683TRP-687ILE-701 MET-704 LYS-708ARG-709 VAL-712GLY-715 GLN-716ALA-722
L-03	TYR-683 MET-703 GLN-716		PHE-719	LEU-625PHE-629ILE-682PHE-686PRO-702MET-704LYS-708ARG-709GLU-711 VAL-712GLN-714 GLY-718VAL-723
L-04	TYR-683 MET-703 GLN-716	GLU-685 GLU-689		TYR-514 HIS-515HIS-557SER-561THR-623ASP-664 SER-667VAL-668PRO-702 MET-704VAL-712
L-05	ASN-562	GLU-689	HIS-515	TYR-514 GLY-559 SER-561 MET-581THR-



		MG-2	PHE-560	623ASP- 664SER-667GLU-685PHE-686MET-704GLY- 715 GLN-716PHE-719
L-06	TYR-683  MET-703 GLN-716		PHE-719	LEU-625PHE-629ILE-682PHE-686ILE- 701PRO-702 LYS-708ARG-709GLU-711 VAL-712GLY-718
L-07	TYR-683  MET-703 GLN-716		PHE-719	HIS-515HIS-557SER-561ASN-562LEU- 625LEU-665 SER-667VAL-668PHE-686ILE-701GLY- 715GLY- 718ALA-722VAL-723
L-08	TYR-683 GLN-703 GLN-716		PHE-719	LEU-625PHE-629LEU-665SER-667VAL-668 PHE-686LYS-708GLU-711 VAL-712GLN-714 VAL-723
L-09	TYR-683  MET-703 GLN-716		PHE-719	ASP-624LEU-627PHE-629LEU-665SER- 668VAL- 668ILE-701GLY-715GLY-718ALA-722
L-10	TYR-683			HIS-515TYR-519HIS-557HIS-553ASP-554GLU- 582 HIS-625THR-623SER-667 VAL-668PHE- 686TRP- 687PRO-702 LYS-708ARG-709GLY-715 GLN- 716
L-11	LYS-708 GLU-711			SER-561PHE-629LEU-665TYR-683PHE-686 TRP-687MET-704ARG-709 VAL-712GLY-715 GLN-716PHE-719
L-12	TYR-683			TRP-687ILE-701LYS-708ARG- GLN-714



				709
	MET-703			GLN-716GLY-718
<b>L-13</b>	TYR-683		PHE-719	ILE-682PHE-686PRO-702LYS-708GLU-711VAL-712ASN-721
	GLN-714			
	GLY-715			
	GLN-716			
<b>L-14</b>	TYR-683			TYR-514HIS-515LEU-625PHE-629 LEU-665
	MET-703			TRP-687ILE-701LYS-708 ARG-709GLY-715
	GLN-716			PHE-719VAL-723
<b>L-15</b>	HIS-515			TYR-514SER-563GLY-559SER-561 MET-581
	ASN-562			THR-623ASP-624LEU-625 ALA-626PHE-629
				LEU-665GLU-685 GLU-689ILE-701PHE-719

Asparagine (ASN),Tryptophan (TRP),Leucine (LEU),Phenylalanine (PHE),Tyrosine (TYR),Lysine (LYS),Glutamine (GLU), Proline (PRO), Threonine (THR), Serine (SER), Glycine (GLN), Methionine (MET), Arginine (ARG), Glutamine (GLY),Alanine (ALA).

Between hydrophobic and nonpolar parts of the ligand, the following residues are among those with

<b>L-16</b>	TYR-683MET-703GLN-716	HIS-515ASP-554GLU-582	PHE-560PRO-702GLU-711	SER-557GLY-559SER-561ASN-562MET-581PHE-629ALA-679 TRP-687 GLU-689MET-704LYS-708ARG-709 GLY-715VAL-723
-------------	-----------------------	-----------------------	-----------------------	---

which selected sixteen ligand compound forms Vander Waals Interactions, TYR-514,HIS-515,LEU-625,PHE-629,LEU-665,VAL-668,ILE-701,GLY-718,TYR-720,VAL-723. The appealing forces are a part of Vander Waals interactions between atoms'electron Clouds and serve a vital part in keeping ligand-receptor interactions active by adding to the complex's overall stability through interactions, with the residues HIS-515, ASN -582, TYR-603, TYR-683, MET-703, TYR-714, GLY-715,GLY-716.

Selected sixteen ligand compound creates hydrogen bond interactions with VAL-1533, it interacts hydrophobically. With the residues PHE-686, PRO-702, GLU-711, it displays enticing charge Interactions. It manifests itself TYR-514,HIS-515,LEU-625,PHE-629,LEU-665,VAL-668,ILE-701,PRO-702,GLY-718,TYR-720,VAL-723and Vander Waals interactions residues.

**Table 2: Dand 3D interaction images of selected derivatives with TSPO protein.**

Compound	2DINTERACTION	3DIMAGE	2D PRODUCEDCOMP LEX
L-01			
L-02	<p><small>Interaktionstypen</small>  <span style="color: green;">■</span> von der Wirtszelle  <span style="color: red;">■</span> von dem Liganden  <span style="color: blue;">■</span> von beiden</p>		
L-03			
L-04			
L-05			
L-06			
L-07			
L-08			

L-09			
L-10			
L-11			
L-12			
L-13			
L-14			
L-15			
L-16			

### [C] - Physicochemical, Pharmacokinetics, drug likeness prediction of selected compound -

The analysis of drug likeness properties in particular ADME, which is for absorption, distribution, metabolism & excretion to determine their effectiveness in the body. An investigation of the ADME qualities of an ensemble of molecules was conducted to ascertain the molecules drug similarity and



physicochemical interactions with the target. It was carried out to support drug research and design with the range of 133.69 to 155.19 molar refractivity (MR). A well-balanced combination of polar and non-polar features is suggested by the MR range of 133.69 to 155.19, which may be helpful for materials that resemble pharmaceuticals. The range of the water solubility (LogS) parameter is -3.97 to -5.82 moles per liter. Most of the ligands on the ADME table have anticipated log S value larger than 2.5, indicating high water solubility. The top poses having good docking score were screened which came under the lipophilicity range (LogP) 2.41 to 4.54. It possesses a high lipophilicity, indicating a great affinity for non-aqueous environments including membranes and lipid bilayers. This range indicates high membrane permeability and potential for oral absorption, but may cause challenges with aqueous solubility and clearance. The topological polar surface area (TPSA) range of 100.12 to 180.45 indicate that the molecule has a moderate to high polar surface area. All molecular weights within the well-known legends are wrong allowed 500 molecular weight range. Molecular weight would be more easily absorbed by diffusion and transferred, in opposition to Lipinski's rule of five. Drug-like ligands ought to contain a maximum ten hydrogen bond acceptors and maximum five hydrogen bond donors. When taken orally, all of the compounds investigated for this investigation were discovered to fit this area, indicating they are presumably very absorbent or porous.

P-group substrate is used to refer to any substance that P group recognizes and transports a particular class of protein called P-group works to stop hazardous chemicals from entering the body which was found in many organs including the liver kidney and brain. P-group levels fluctuate along the gut which may be advantages when creating medications with a delayed release. Tend to be extremely lipophilicity molecular weight with high number of HBA and HBD.

**Table-** Pharma cokinetics and drug-likeness properties of selected derivative so fPDE10A.

Compound	MW	HBA	HBD	MREFR	TPSA	LOGP	LOGS	BBB	P-GRO	DRUG LIKE	CYP1 A2IN	CYP2 C9IN
				ACTIVITY					UPSU	NESS	HIBITHIBI	TORS
									BSTR	ORS		
									ATE			
L-01	511.61	3	6	140.97	143.72	2.98	-4.01	No	Yes	1	No	No
L-02	589.52	1	6	149.17	108.91	4.54	-5.47	No	Yes	1	No	Yes
L-03	496.6	2	6	136.57	117.7	3.66	-4.35	No	Yes	0	No	Yes



L-04	526.62	2	7	143.49	129.14	3.49	-4.42	No	Yes	1	No	No
L-05	498.57	4	7	133.69	146.72	3.12	-4.02	No	Yes	0	No	No
L-06	512.6	3	7	138.59	137.93	3.31	-4.22	No	Yes	1	No	No
L-07	569.65	0	8	155.19	145.94	3.86	-4.83	No	No	2	No	Yes
L-08	526.62	2	7	143.49	129.14	3.49	-4.42	No	Yes	1	No	No
L-09	486	6	1	131.68	122.3	3.48	-5.82	No	Yes	0	No	No
L-10	525.64	2	6	145.87	134.93	3.16	-4.2	No	Yes	1	No	No
L-11	510.63	2	6	141.53	117.7	4.03	-4.66	No	Yes	1	No	Yes
L-12	539.67	1	6	150.78	126.14	3.35	-4.4	No	Yes	1	No	No
L-13	576.66	3	9	146.43	180.45	2.41	-3.97	No	Yes	2	No	No
L-14	561.47	3	6	139.37	126.49	4.17	-5.07	No	Yes	1	No	Yes
L-15	538.68	0	6	151.34	100.12	4.39	-5.05	No	No	1	No	Yes
L-16	589.52	1	6	149.17	108.91	4.54	-5.47	No	Yes	1	No	Yes

Molecular weight (MW), hydrogen bond acceptor (HBA), hydrogen bond donor (HBD), molar refractivity (M-REFRACTIVITY), rotatable bond (ROT), topological polar surface area (TPSA), partition coefficient (LOGP), solubility (LOGS), blood brain barrier (BBB), P-Group Substrate; CYP1A2 INHIBITOR & CYP2C19 INHIBITOR types of cytochrome inhibitors.

#### [D] – QSAR Result and Discussion–

##### MW Vs HBD

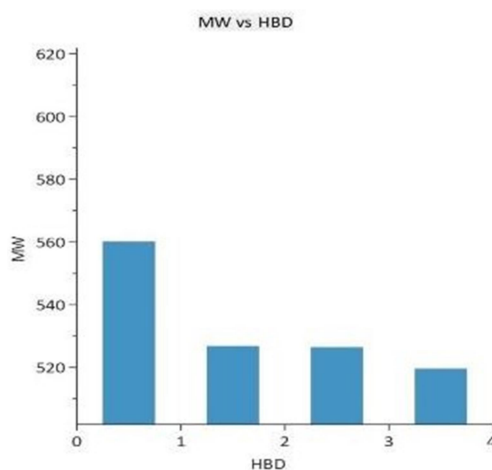


**Fig. 1 - Molecular Weight Vs Hydrogen Bond Donor**

A moderate to the compounds under research is indicated by the compounds lying in the HBD range of 3 to 4 range is particularly suitable to molecules with a molecular weight of less than 500, indicating that the analysis focuses on relatively tiny molecules. These chemical substances can enter the brain.

**HBDVsMW**

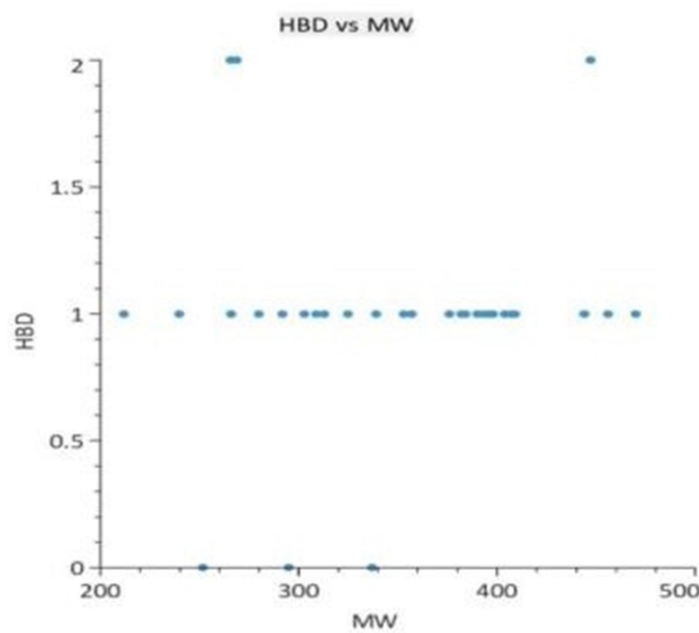


**Fig. 2 - Hydrogen Bond DonorVs Molecular Weight**

The compounds in the HBD range of 0 to 1 are particularly appropriate to molecules with a molecular weight of less than 500, indicating that the analysis concentrates on relatively small molecules. This is demonstrated by the compounds in this range being moderate to the chemicals under study molecules. These chemicals can go into the brain.

### MWVs Lipinski Rule of Five

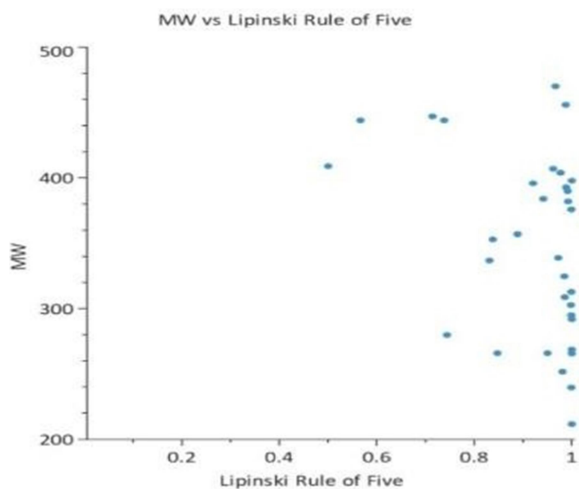


**Fig. 3 - Molecular Weight Vs Lipinski Rule of Five**

The Lipinski Rule of Five roughly applies to all compounds, indicating that they all have the necessary drug-like qualities. The solubility, cell permeability, and overall drug-like properties of molecules with moderate lipophilicity in this molecular weight range are typically increased. Showing to their qualities falling inside the desirable range of log BB, were able to cross BBB. i.e., 0.5 to 1.

### MW Vs TPSA

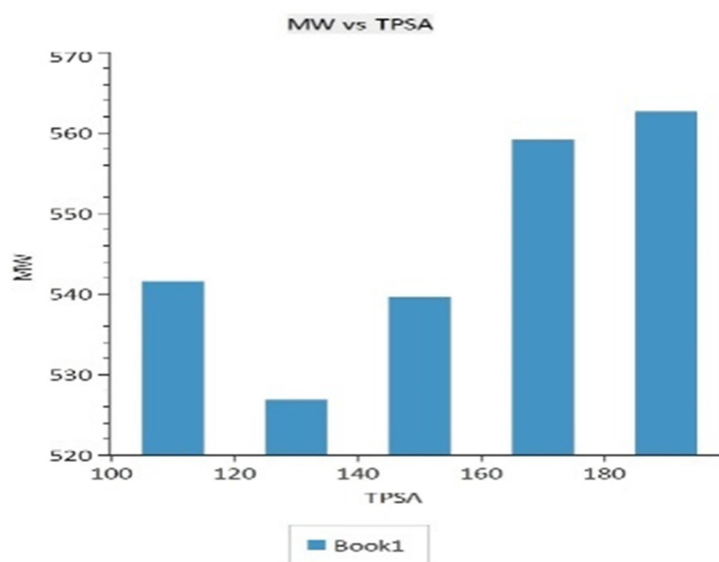


**Fig. 3 - Molecular Weight Vs Topological Surface Area**



TPSA and a compound absorption properties were found with the help of StarDrop. Increased water solubility and better oral absorption result from higher TPSA values. More polar groups on the molecule surface are indicated by a bigger TPSA, which enhances the performance of the molecule interplay with the digestive tracts water environment. Nevertheless, excessive decreased membrane permeability may result from elevated TPSA values as well. Several substances those molecules with molecular weights between 400 and 550 g/mol or within the specified range, were having a higher number of polar groups, so that their TPSA values are more than 120 which leading to decrease.

### **Conclusion & Future Aspect -**

In conclusion, this study investigated the binding affinity and pharmacokinetic properties of selected molecules using molecular docking and ADME profiling techniques. The results showed that L-1 to L-16 ligands exhibited strong binding affinity to the PDE10 A protein and interacted with key residues in the active site through hydrogen bonding. All identified ligands had a molecular weight within the acceptable range and most of them had aqueous solubility. However, some ligands may have limited slow penetration through blood brain barrier. Overall, the findings suggest that the identified molecules have potential for further development as drugs for the treatment of disease related to PDE10 A inhibitors.

The drug discovery industry is undergoing a significant transformation due to the swift progress in biomarker testing technology and the human genome projects. AI is set to revolutionize this field by introducing novel, efficient, and cost-effective approaches to drug discovery. AI can rapidly analyze vast amounts of data, identify suitable targets and ligands, design and execute experiments, and optimize drug development. Moreover, structure-based drug discovery, which utilizes the knowledge of biological molecules 3D structures, improves drug design and development outcomes. By utilizing advanced structural biology techniques, researchers can identify new therapeutic targets and develop effective drugs, leading to significant advancements in drug discovery.

### **References**

1. Ferreira, L.G., Dos Santos, R.N., Oliva, G., & Andricopulo, A.D. (2015). Molecular docking and structure-based drug design strategies. *Molecules (Basel, Switzerland)*, 20(7), 13384–



- 13421.<https://doi.org/10.3390/molecules200713384>
2. Sadybekov, A. V., & Katritch, V. (2023). Computational approaches streamlining drug Discovery. *Nature*, 616(7958), 673–685. <https://doi.org/10.1038/s41586-023-05905-z>
  3. Tabeshpour, J., Sahebkar, A., Zirak, M. R., Zeinali, M., Hashemzaei, M., Rakhshani, S., & Rakhshani, S. (2018). Computer-aided Drug Design and Drug Pharmacokinetic Prediction: A Mini-review. *Current pharmaceutical design*, 24(26), 3014–3019. <https://doi.org/10.2174/1381612824666180903123423>
  4. Tautermann C.S. (2020). Current and Future Challenges in Modern Drug Discovery. *Methods In molecular biology (Clifton, N.J.)*, 2114, 1–17. [https://doi.org/10.1007/978-1-0716-0282-9\\_1](https://doi.org/10.1007/978-1-0716-0282-9_1)
  5. Stanzione, F., Giangreco, I., & Cole, J. C. (2021). Use of molecular docking Computational Tools in drug discovery. *Progress in medicinal chemistry*, 60, 273–343. <https://doi.org/10.1016/bs.pmch.2021.01.004>
  6. Rock, B. M., & Foti, R. S. (2019). Pharmacokinetic and Drug Metabolism Properties of Novel Therapeutic Modalities. *Drug metabolism and disposition: the biological fate of Chemicals*, 47(10), 1097–1099. <https://doi.org/10.1124/dmd.119.088708>
  7. Schneider, N., Lange, G., Hindle, S., Klein, R., & Rarey, M. (2013). A consistent Description Of Hydrogenbond and Dehydration energies in protein-ligand complexes: Methods behind the HYDE scoring function. *Journal of computer-aided molecular Design*, 27(1), 15–29. <https://doi.org/10.1007/s10822-012-9626-2>
  8. Bazzoli, A., & Karanicolas, J. (2017). “Solvent hydrogen-bond occlusion”: A new model Of Polar desolvation for biomolecular energetics. *Journal of computational Chemistry*, 38(16), 1321–1331. <https://doi.org/10.1002/jcc.24740>
  9. González-Díaz H. (2008). Quantitative studies on Structure-Activity and Structure-Property Relationships (QSAR/QSPR). *Current topics in medicinal chemistry*, 8(18), 1554. <https://doi.org/10.2174/156802608786786615>
  10. Vucicevic, J., Nikolic, K., & Mitchell, J. B. O. (2019). Rational Drug Design of Antineoplastic Agents Using 3D-QSAR, Cheminformatics, and Virtual Screening Approaches. *Current medicinal chemistry*, 26(21), 3874–3889. <https://doi.org/10.2174/0929867324666170712115411>
  11. Abdolmaleki, A., Ghasemi, J. B., & Ghasemi, F. (2017). Computer Aided Drug Design For Multi-Target Drug Design: SAR /QSAR, Molecular Docking and Pharmacophore Methods. *Current drug targets*, 18(5), 556–575. <https://doi.org/10.2174/1389450117666160101120822>



12. Fang, C., & Xiao, Z. (2016). Receptor-based 3D-QSAR in Drug Design: Methods and Applications in Kinase Studies. *Current topics in medicinal chemistry*, 16(13), 1463–1477.  
<https://doi.org/10.2174/1568026615666150915120943>
13. Ginex, T., Vazquez, J., Gilbert, E., Herrero, E., & Luque, F. J. (2019). Lipophilicity in Drug Design: an overview of lipophilicity descriptors in 3D-QSAR studies. *Future Medicinal Chemistry*, 11(10), 1177–1193. <https://doi.org/10.4155/fmc-2018-0435>
14. Abdolmaleki, A., Ghasemi, J. B., & Ghasemi, F. (2017). Computer Aided Drug Design For Multi-Target Drug Design: SAR/QSAR, Molecular Docking and Pharmacophore Methods. *Current drug targets*, 18(5), 556–575. <https://doi.org/10.2174/1389450117666>
15. Stanzione, F., Giangreco, I., & Cole, J. C. (2021). Use of molecular docking Computational Tools in drug discovery. *Progress in medicinal chemistry*, 60, 273–343. <https://doi.org/10.1016/bs.pmch.2021.01.004>
16. Saikia, S., & Bordoloi, M. (2019). Molecular Docking: Challenges, Advances and its Use In Drug Discovery Perspective. *Current drug targets*, 20(5), 501–521. <https://doi.org/10.2174/1389450119666181022153016>
17. Abdolmaleki, A., Ghasemi, J. B., & Ghasemi, F. (2017). Computer Aided Drug Design For Multi-Target Drug Design: SAR/QSAR, Molecular Docking and Pharmacophore Methods. *Current drug targets*, 18(5), 556–575. <https://doi.org/10.2174/13894501176661601011208>
18. Shankar, R., Joshi, M., & Pathak, K. (2018). Lipid Nanoparticles: A Novel Approach for Brain Targeting. *Pharmaceutical nanotechnology*, 6(2), 81–93. <https://doi.org/10.2174/221173850666618061110041>
19. Deep, O., & Zhou, J. (2023). In silico Methods for Drug Design. *Current topics in Medicinal Chemistry*, 23(3), 155–157. <https://doi.org/10.2174/1568026623666221206093350>
20. Scotti, L., & Scotti, M. T. (2020). Recent Advancement in Computer-Aided Drug Design. *Current pharmaceutical design*, 26(15), 1635–163. <https://doi.org/10.2174/138161282615200518092124>
21. Koss, J., Rheinlaender, A., Truebel, H., & Bohnet-Joschko, S. (2021). Social media Mining In Drug development-Fundamentals and use cases. *Drug discovery today*, 26(12), 2871–2880. <https://doi.org/10.1016/j.drudis.2021.08>